Lipid bilayer surface association of lung surfactant protein SP-B, amphipathic segment detected by flow immunofluorescence

Marjorie L. Longo, Alan Waring,* and Joseph A. N. Zasadzinski

Department of Chemical and Nuclear Engineering, University of California, Santa Barbara, California 93106; and *Department of Pediatrics, King/Drew Medical Center and University of California, Los Angeles, School of Medicine, Los Angeles, California 90059 USA

ABSTRACT Lung surfactant protein, SP-B, and synthetic amphipathic peptides derived from SP-B were studied in model lung surfactant lipid bilayers by immunofluorescent labeling. Liposomes were formed by hydrating a lipid film on the glass viewing port of a temperature controlled flow chamber. Membrane associated peptides were detected by epifluorescence optical microscopy of the binding of anti-peptide polyclonal monospecific antibodies and FITC-conjugated secondary antibodies added to buffer contained in the flow chamber. Liposomes were bound by antibody to residues 1-25 of SP-B if formed from lipid films containing the 1-25 peptide, (SP-B(1-25)), or if SP-B(1-25) was added to already formed liposomes in buffer solution. The distribution of antigen-antibody complex was temperature dependent with aggregation occurring at ≥30°C. Surface association was not detected in liposomes formed from lipid films containing the 49-66 peptide (SP-B(49-66)), using an antibody to the 49-66 peptide, or to a synthetic version of the SP-B protein, (SP-B(1-78)), using both antibodies to the 49-66 peptide and the 1-25 peptide. The detection of SP-B(1-78) with antibody to the 49-66 sequence was only possible after reducing SP-B(1-78) with dithiothreitol, suggesting that the COOH-terminus of the full monomer protein is accessible to the bulk aqueous environment unlike the COOH-terminal peptide. The size, number of layers, and fluidity of the liposomes were not altered by protein or peptides, although they were affected by lipid composition and temperature.

INTRODUCTION

A mixture of lipids and proteins, commonly known as lung surfactant, lines the airspaces of the lungs of all mammalian species. This mixture stabilizes the lung alveoli during breathing by varying the air-surfactant interfacial tension according to alveolar curvature, ensuring that alveoli neither collapse nor rupture. The interfacial tension is changed by rapid adsorption, desorption, and compression of surfactant at the air-surfactant interface during each breathing cycle (1–3). Lung surfactant contains at least four specific proteins: SP-A, SP-B, SP-C, and SP-D (4, 5), along with several lipid species, primarily dipalmitoylphosphatidylcholine, phosphatidylglycerol, phosphatidylinositol, and phosphatidylethanolamine. SP-B and SP-C are low molecular weight hydrophobic proteins with reduced molecular weights of 5 and 3.5 kD, respectively, that appear to be important to surfactant function in vivo (6). These proteins co-isolate with lipid extract of surfactant prepared by chloroform-methanol extraction, and enhance adsorption of surfactant lipids to an air-water interface in vitro (7–10). Premature infants with insufficient amounts of lung surfactant suffering from Respiratory Distress Syndrome (RDS) have been successfully treated with exogenous surfactants that contain SP-B and SP-C extracted from animal or human sources (8, 11–13). Other surfactant therapies mix bovine or porcine SP-B and SP-C with synthetic lipids or extracted lung lipids (6, 14–17), also with reasonable success. However, the detailed role of SP-B or SP-C in enhancing surfactant function is still not well understood.

The association with surfactant molecules and structure in lipids of SP-B and its amphipathic peptides have been studied using several model lipid mixtures and by various physical measurements. We have focused on the study of two amphipathic peptides of SP-B based on published sequence data for human SP-B (18–21). These synthesized domains include the NH_2-terminal residues 1-25, which are known as SP-B(1-25), and the COOH-terminal residues 49-66, which are called SP-B(49-66). Compared with lipid alone, mixtures of SP-B(1-25) and SP-B(49-66) in lipid had lower minimum surface tensions and higher rates of surface adsorption (22, 23). SP-B(1-25) has a high affinity for negatively charged lipid monolayers and readily inserts into negatively charged lipid monolayers (22). The surface activity of SP-B(1-25), SP-B(49-66), and synthetic whole SP-B(1-78) has been correlated with their secondary structures in membrane mimicking and synthetic surfactant lipid environments. Circular Dichroism (CD) and Fourier Transform Infra-Red (FTIR) Spectroscopy of surfactant lipid-peptide multilayer films indicate that the SP-B peptides assume largely helical conformations in membrane environments (22, 24, 25). The association of enhanced surface activity and high helical secondary structure for these peptides in membrane mimic environments is consistent with the observation that these peptides consist of elements predicted to be amphipathic by the alpha hydrophobic moment analysis (26) of the SP-B amino acid sequence (23, 27). The coordinates for the SP-B sequences locate the SP-B amphipathic segments in the surface sector of the hydrophobic moment plot near lytic peptides such as Magainin and Melittin, suggesting that the polar component of the amphipathic sequences may have hydrophilic surface accessibility in surfactant lipid dispersions and detergent micelles.

Immunostaining experiments have been used to detect SP-B by anti-peptide antibodies to determine sur-

Address correspondence to Joseph Zasadzinski.

0006-3495/92/09/760/14 $2.00

face accessibility to antibody and conformational (disulfide linkage) differences between amphipathic peptides and native protein (24). A continuous region of the whole protein is surface accessible if an antibody directed at a synthetic peptide of the region successfully binds the protein (28). Binding does not occur if the directed region is buried in the hydrophobic core of the protein due to the protein configuration (29). As expected, antibodies directed against specific peptides identified those peptides. However, antibody directed against SP-B(1-25) identified monomeric native SP-B (MW = 8 kD) but did not identify oligomeric native SP-B (MW = 17 and 26 kD). This suggests that the 1-25 region of native monomeric SP-B is surface-accessible and closely approximates the configuration of SP-B(1-25) peptide. Antibody directed against SP-B(49-66) identifies both oligomeric and monomeric forms of native SP-B, suggesting that this domain is readily accessible in both the oxidized and reduced form (24). However, preliminary results showed that antibody directed against SP-B(1-25) did not bind synthetic monomeric or oligomeric SP-B(1-78). Antibody directed against SP-B(49-66) did not bind to synthetic oligomeric SP-B(1-78), but did bind to monomeric SP-B(1-78). Hence, the conformation of the synthetic protein is likely to be different than the native protein, especially in the NH_2-terminus region or 1-25 region.

Immunostaining techniques, however, fail to provide information on the location of these low molecular weight proteins in membranes and their ability to spontaneously associate with bilayers. It is also difficult to predict, using only data from immunostaining experiments, if the 1-25 or 49-66 sequences of SP-B(1-78) or the synthetic peptides are accessible to antibody in a lipid environment. In immunostaining, protein to be identified by antibody is adsorbed to a hydrophobic blotting membrane with an aqueous solvent (30) and may be associated with residual sodium dodecyl sulfate from electrophoresis. To better assess the accessibility of the protein in its native lipid environment, it is necessary to examine antibody binding in a more realistic model lipid membrane system. In our technique, which we call flow immunofluorescence, giant vesicles are formed by slow swelling of a dried lipid film with buffer in a temperature controlled flow chamber. The giant vesicles within the micro-flow chamber are easily viewed in the optical microscope without additional preparation or extraction. Peptides and proteins are detected in the vesicle bilayer by the attachment of polyclonal monospecific antibodies. FITC (fluorescein isothiocyanate)-conjugated secondary antibodies are then used to visualize the association in the epifluorescence microscope. Similar assays have been used to determine the molecular topography of proteins associated with reconstituted cell membranes (31–33).

In addition to studies of proteins and peptides within bilayers, flow immunofluorescence is also quite useful to determine membrane binding characteristics of water soluble proteins. Since SP-B(1-25) is water soluble, this system is well suited for the injection of SP-B(1-25) into preformed vesicle solutions of various composition to detect peptide insertion into lipid bilayers. Of particular interest is the affinity of SP-B(1-25) (which is positively charged at neutral pH as it contains two lysine and two arginine residues) to neutral dipalmitoylphosphatidylcholine (DPPC) vesicles, DPPC/egg phosphatidylglycerol (PG) vesicles, and DPPC/palmitic acid vesicles. We can also observe vesicles of different lipid compositions through the flow chamber to examine composition dependent shape changes and peptide-antibody complex redistribution with temperature or composition. We make general correlations between vesicle shape, effectiveness, and composition using this simple visualization technique. In this fashion, we have determined a significant role of the lipid species in forming an effective lung surfactant.

TABLE 1 Amino acid sequences of synthetic SP-B peptides and synthetic SP-B that were used for studies*

SP-B(1-25)
FPIPLPYCWLCRALIKRIQAMIPKG
1 *25*

SP-B(49-66)
LAERYSVILLDTLLGRN1‡LCONH$_2$§
49 *66*

SP-B(1-78)
FPIPLPYCWLCRALIKRIQAMIPKGALRVA *30*
VAQVCRVVPLVAGGICQCLAERYSVILLDT *60*
LLGRMLPQLVCRLVLRCS *78*

* Residues are numbered from the NH_2-terminus.
‡ N1 is the nonoxidizable methionine analogue, norleucine.
§ $CONH_2$ represents carboxyamidation of the COOH-terminus.

MATERIALS AND METHODS

Chemicals

L-α Dipalmitoylphosphatidylcholine, egg phosphatidylglycerol, and palmitic acid were purchased from Sigma Chemical Co. (St. Louis, MO) and were used without further purification. Dithiothreitol was purchased from Pierce Chemical Co. (Rockford, IL). Fluorescein isothiocyanate (FITC)-conjugated goat anti-rabbit (GAR) antibody was obtained from Orgenon Technica (Durham, NC).

Peptide synthesis

Synthetic peptides representing the NH_2-terminal amino acid sequence (residues 1-25), the COOH-terminus (residues 49-66), and full length SP-B (residues 1-78) (Table 1) were synthesized at the UCLA Peptide Synthesis Facility. The SP-B(1-25) segment and the SP-B(49-66) segment were synthesized using the Merrifield method employing a BOC strategy (23, 34). Full length SP-B(1-78) was synthesized also using the solid phase method with BOC protected amino acids (25). The crude peptides were purified by C4 (Vydac, C4) reverse phase HPLC using a water-acetonitrile gradient containing 0.1% trifluoroacetic acid. HPLC solvents and ion pairing agents were removed from the purified peptides by vacuum centrifugation. The expected molecular mass for SP-B(1-25) and SP-B(49-66) was obtained by FAB-Mass Spectrometry

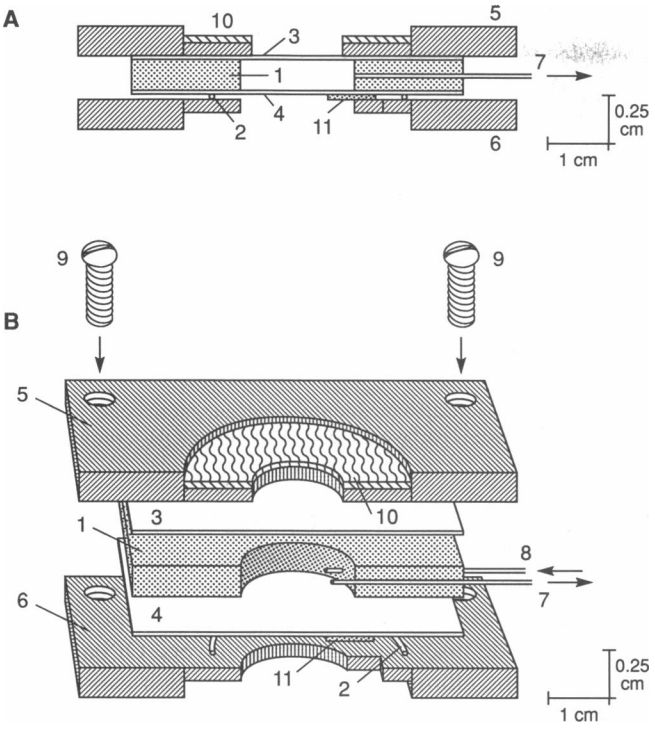

FIGURE 1 Temperature controlled micro-flow chamber used in immunofluorescence experiments. The chamber is made by sandwiching a teflon spacer [*1*], an o-ring [*2*], and two glass cover slips [*3, 4*] between two black anodized plates [*5, 6*]. Liposomes formed in the solution volume between the two cover slips remain attached to the bottom cover slip as buffer solutions are exchanged through inlet and outlet capillaries [*7, 8*]. The solution volume is temperature controlled by an attached thermofoil heater [*10*] and resistive temperature probe [*11*]. (*A* and *B*) Cross-sectional views of flow chamber (scales in *X* and *Y* direction are different).

(City of Hope Mass Spectrometry Facility, Duarte, CA). The amino acid sequence for synthetic SP-B(1-78) was confirmed by sequencing the peptide from residue 1 to 78 with an ABI 470A protein sequencer (25) and the expected molecular mass was obtained by electrospray mass spectroscopy (NPI Analytical Chemistry Facility).

Antibodies to synthetic peptides

For preparation of anti-SP-B(1-25) and SP-B(49-66) antibodies, New Zealand White rabbits were injected with 200 μg of peptide, in the presence of Freund's adjuvant (24). After 3 wk, the rabbits were given a booster injection with 500 μg of incomplete Freund's adjuvant. The animals were bled 11 d after the last immunization. Synthetic peptides were injected into rabbits in Freund's adjuvant without conjugation so as not to alter the antigenic properties of the peptide moiety (35).

Temperature controlled flow chamber

The flow immunofluorescence chamber (Fig. 1) is constructed by sandwiching a Teflon spacer [*1*], an o-ring [*2*], and two glass cover slips [*3, 4*] between two black anodized aluminum plates [*5, 6*]. The top and bottom plates have a through hole at their centers, 1.5 cm and 2 cm in diameter, respectively, as a viewing port and to allow the objective lens to seat close to the glass cover slip. The Teflon spacer has two closely spaced inlet and outlet capillaries [*7, 8*] (26 gauge stainless steel needle bores) used for exchange of rinse buffers and buffer containing peptide or antibodies. The whole assembly is held together by four screws through the aluminum plates [*9*]. The exchange volume is small (0.3 ml), which allows for the use of very little antibody solution. Temperature regulation from 20 to 50°C is achieved by an attached thermofoil heater (HK 5542 R25.5) [*10*] and resistive temperature probe [*11*] (S651; Minco, Minneapolis, MN) controlled by a microprocessor-based temperature controller (CN 9000; Omega, Stamford, CT). The heater is placed in a depression on the aluminum plates so as to minimize the amount of aluminum heated. The temperature probe is held with adhesive to the glass on the opposite side of the heater. The time required to heat the buffer contained in the chamber from room temperature to 43°C is ~5 min. Temperature control of ±0.1°C was easily achieved after properly tuning the controller. The temperature gradient across the water-filled sample chamber, while the chamber was held at 43°C, was measured by affixing an additional resistive temperature probe to the glass on the heater side and measuring the resistivity of both temperature probes. The temperature difference between the top and bottom cover glass was <1°C. This chamber is similar in concept to a measuring chamber used to visualize the incorporation of K-1 antigen into giant liposomes (36). The main difference is that the temperature control of the chamber described here is much more compact; temperature control is obtained by an easily portable controller and heater rather than a water bath. Our design also has the advantage that the Teflon spacers can easily be made of different thicknesses and the sample touches only glass, Teflon, and the stainless steel needle bores. Buffer solutions were injected into the chamber slowly (0.5 ml/min) through (0.025 in ID) HPLC tubing (Becton Dickinson and Company, (Parsippany, NJ) with a syringe pump (341B; Orion, Boston, MA).

Formation of giant liposomes

In a typical experiment, 2.55 mg DPPC, 0.79 mg egg PG, 0.30 mg palmitic acid (this ratio of DPPC:PG:PA is called Tanaka lipids (9)), and 0.11 mg SP-B peptide were dissolved in 0.5 ml of chloroform:methanol (2:1 vol:vol) solution. Small drops (<0.5 μl) of the chloroform/methanol solution containing the desired lipid mixture were then deposited on a cover slip and the solvent removed by a stream of dry nitrogen gas followed by several hours under moderate vacuum. The cover slip was then placed into the flow immunofluorescence chamber which was then assembled and filled with room temperature 10 mM phosphate buffered normal saline (PBS), with 0.5% bovine serum albumin (BSA) at pH 7.2. The chamber temperature was raised to 43°C (above the 41°C gel-liquid crystal transition temperature of DPPC (37)) and the lipid was allowed to swell for 1 h during which time giant vesicles formed. Below this temperature, giant vesicles were slow to form. The heater was then turned off so that the chamber returned to room temperature. The vesicles formed in this fashion generally did not detach from the glass cover slip during exchange of solution at room temperature, perhaps because predominantly DPPC bilayers are relatively rigid below the gel-fluid phase transition of the lipid. The formation of mainly uni- or multi-lamellar vesicles depended upon the composition of the lipid film deposited.

Microscopy

Microscopic observations were performed using an Olympus IMT-2 Inverted Research Microscope with a 40× lens (Olympus long working distance, CD Plan 40 PL, numerical aperture 0.6). The microscope could be operated in either epifluorescence or differential interference contrast (Nomarsky) modes. Images were recorded with an Olympus OM-2, 35 mm camera using TMAX 400 ASA and Ektachrome 800/1600 ASA films (Kodak, Rochester, NY). Kodak Polycontrast III RC paper was used for prints.

RESULTS AND DISCUSSION

Surface association of SP-B(1-25) in giant liposomes

Giant vesicles were hydrated from Tanaka lipids and SP-B(1-25) as discussed above, then polyclonal rabbit anti-

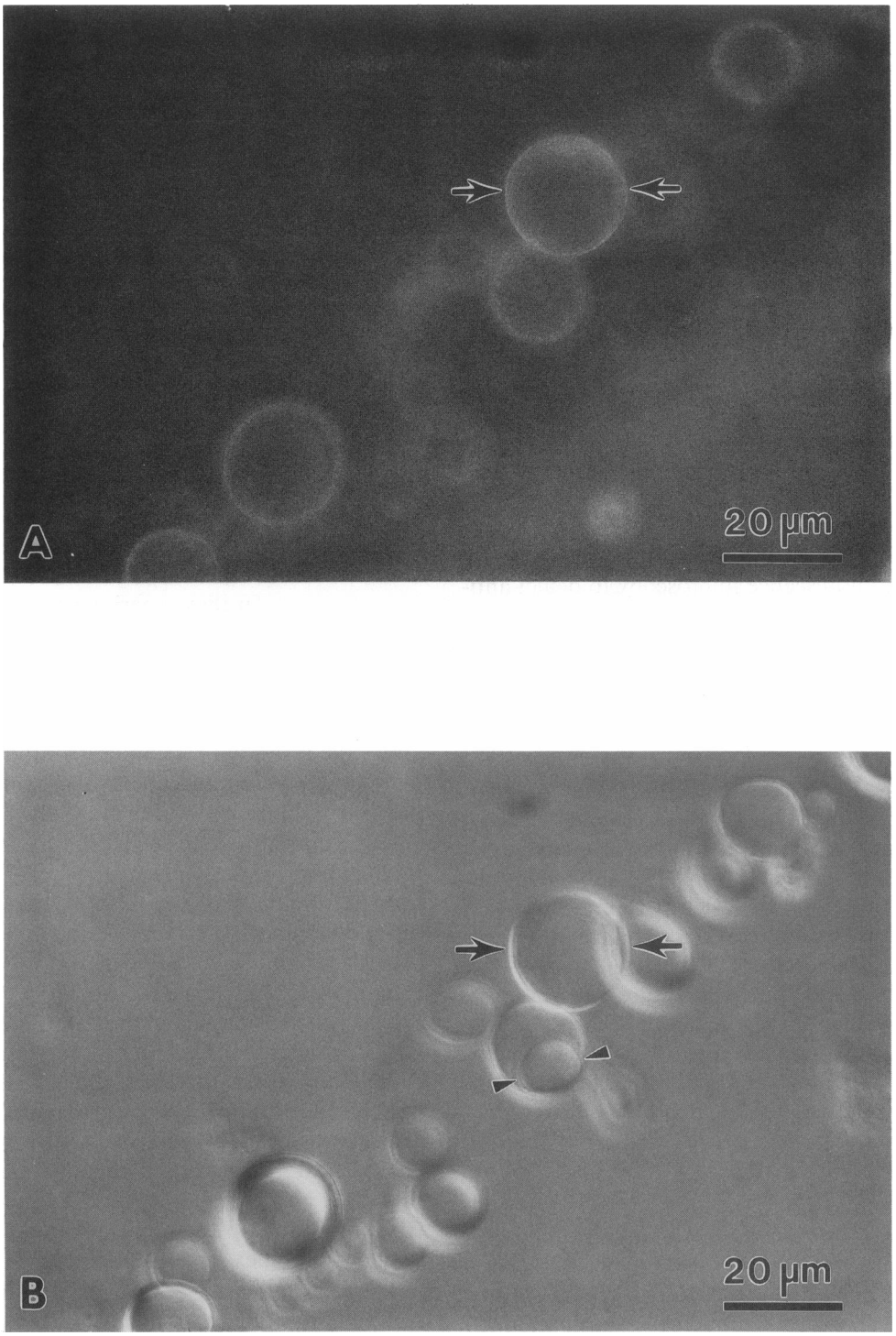

FIGURE 2 (*A*) Epifluorescence image of labelling (*large arrows*) corresponding to binding of antibody (FITC-conjugated goat anti-rabbit [GAR] antibody and polyclonal rabbit [PR] anti-SP-B [1-25 antibody]) to Tanaka lipid bilayer associated SP-B(1-25). (*B*) Differential Interference Contrast (DIC) image of giant vesicles. Large arrows indicate lipid bilayer of vesicle corresponding to *A*. The small arrows mark an encapsulated vesicle that has no fluorescence associated with it because the secondary antibody can not penetrate the lipid bilayer.

SP-B(1-25) antibody (50 μg in 400 μl buffer) was injected into the flow chamber. The antibody was incubated with the vesicles containing peptide for 45 min at room temperature. The volume of the flow chamber was then thoroughly exchanged at room temperature with 5 ml buffer (~15 times the chamber volume), and FITC-conjugated GAR antibody (50 μg in 400 μl buffer) was injected into the chamber. After incubation at room temperature for 45 min, the chamber volume was exchanged again with 5 ml of buffer at room temperature to minimize back-

TABLE 2 **Summary of immunoreactivities between lipid associated synthetic SP-B peptides and synthetic SP-B and two antibodies**

		Antibodies	
Antigen	Lipid	NH_2-terminus	COOH-terminus
SP-B(1-25)	DPPC/egg PG/PA*	yes	—
SP-B(1-25)	DPPC/egg PG	yes	—
SP-B(1-25)	DPPC/PA	yes	—
SP-B(1-25)	DPPC	yes (weak)	—
SP-B(49-66)	DPPC/egg PG/PA	—	no
SP-B(1-78)	DPPC/egg PG/PA	no	no
SP-B(1-78) reduced	DPPC/egg PG/PA	no	yes (diffuse, weak)

* Palmitic acid has been abbreviated as PA.

ground fluorescence. The liposomes were then examined by both differential interference contrast microscopy (DIC) and fluorescence microscopy to detect antigen binding.

Fig. 2 shows a typical result. The fluorescence (*A*) corresponds to binding of antibody to surface associated SP-B(1-25) and is seen as a homogeneous bright ring (*large arrows*) on a dark background. Comparison of this image to the DIC image (*B*) shows that the fluorescence is associated with the external membrane of the giant liposomes (*large arrows*). Vesicles encapsulated inside of giant vesicles can clearly be seen in the DIC image (*B*) (*small arrows*), but fluorescently labelled antibody is not associated with these interior vesicles (*A*), indicating that the antibody is isolated to the surface and can not penetrate the bilayer. The results of all experiments are summarized in Table 2. If the temperature was raised to ~30°C post-labelling, the fluorescence becomes patchy (Fig. 3, *arrows*). Vesicles made from Tanaka lipids without added SP-B(1-25) showed no fluorescence, confirming that the labelling was not due to nonspecific binding.

Insertion of SP-B(1-25) into giant liposomes

Previous CD and FTIR results (22) have shown that SP-B(1-25) preferentially forms an α-helical structure when in the presence of lipids or structure-forming solvent (50% trifluoroethanol, 50% water). Examination of amino acid positions 9 through 26 using a Shiffer-Edmondson analysis (Fig. 4 *A*) showed segregation of polar residues from nonpolar ones in two distinct hemifaces, as is typical of amphipathic sequences (38). We hypothesized that due to this amphipathic nature, SP-B(1-25) added to the chamber solution after vesicle formation would spontaneously associate with the lipid membrane. Therefore, the experimental procedure was modified so that 50 μg of SP-B(1-25) in 400 μl of buffer was added to giant vesicles formed of only Tanaka lipids. After incubation for 45 min at 43°C, the excess peptide was rinsed from the chamber and the vesicles were labelled as described above.

Similarly, vesicles formed from DPPC:egg PG, 2.55:0.79, DPPC:palmitic acid, 2.55:0.30, and pure DPPC (100%) were incubated with 50 μg of SP-B(1-25) in 400 μl of buffer and then labelled. In vesicles formed of Tanaka lipids, DPPC/egg PG and DPPC/palmitic acid, fluorescence was associated with the membranes of these vesicles, indicating that the peptide SP-B(1-25) did spontaneously associate with the vesicle membranes. The fluorescence was often slightly inhomogeneous, especially in comparison with the fluorescence observed in the original preparation in which the peptide was mixed with the lipids before hydration. The inhomogeneity appeared to increase with increasing temperature. Marked inhomogeneities occurred at temperatures above 30°C for all mixtures except vesicles formed solely of DPPC. This patching is similar to a time-dependent inhomogeneous distribution of label seen by Decher (36), which was reported to be due to the use of a different K-1 antigen. However, in that experiment, the observation was done at a temperature (35°C) well above the gel-liquid phase transition of the lipid used (dimyristoylphosphatidylcholine) (36). Hence, it is likely that the inhomogeneities are caused by some attractive interaction between either the primary or secondary antibody, or the entire complex, which can lead to aggregation much more quickly in fluid membranes than in gel membranes.

The fluorescence associated with vesicles formed of DPPC alone (Fig. 5) was much weaker than in vesicles formed from the Tanaka mixture, DPPC/egg PG (Fig. 6) or DPPC/palmitic acid vesicles and appeared to be of an intensity slightly above background. Note that vesicle tubules were also labelled in the DPPC/egg PG mixture (Fig. 6). Increasing the amount of SP-B(1-25) added to DPPC vesicles to 100 μg increased the membrane associated fluorescence to a level similar to that of the mixed lipid vesicles. Upon increasing the temperature, the fluorescence associated with the DPPC vesicles became patchy near the gel-liquid crystal transition of DPPC (~41°C), again suggesting that the inhomogeneities in labelling were due to enhanced lateral diffusion of the antibody complex in the fluid lipids.

The weak fluorescence associated with vesicles formed of DPPC indicates that much less peptide is bound to uncharged DPPC vesicles than to vesicles containing charged lipids. This observation suggests that an electrostatic interaction is necessary for initial binding of peptide to vesicles. A possible explanation for the peptide-charged lipid interaction involves a strong electrostatic attraction between positive residues (2 lysine, 2 arginine) and the negatively charged lipids enhancing the adsorption of SP-B(1-25). Subsequently, when the peptide adsorbs to the lipid surface, it must orient and fold in such a way that the positive residues do not interact with the hydrophobic lipid core. The SP-B(1-25) amphipathic al-

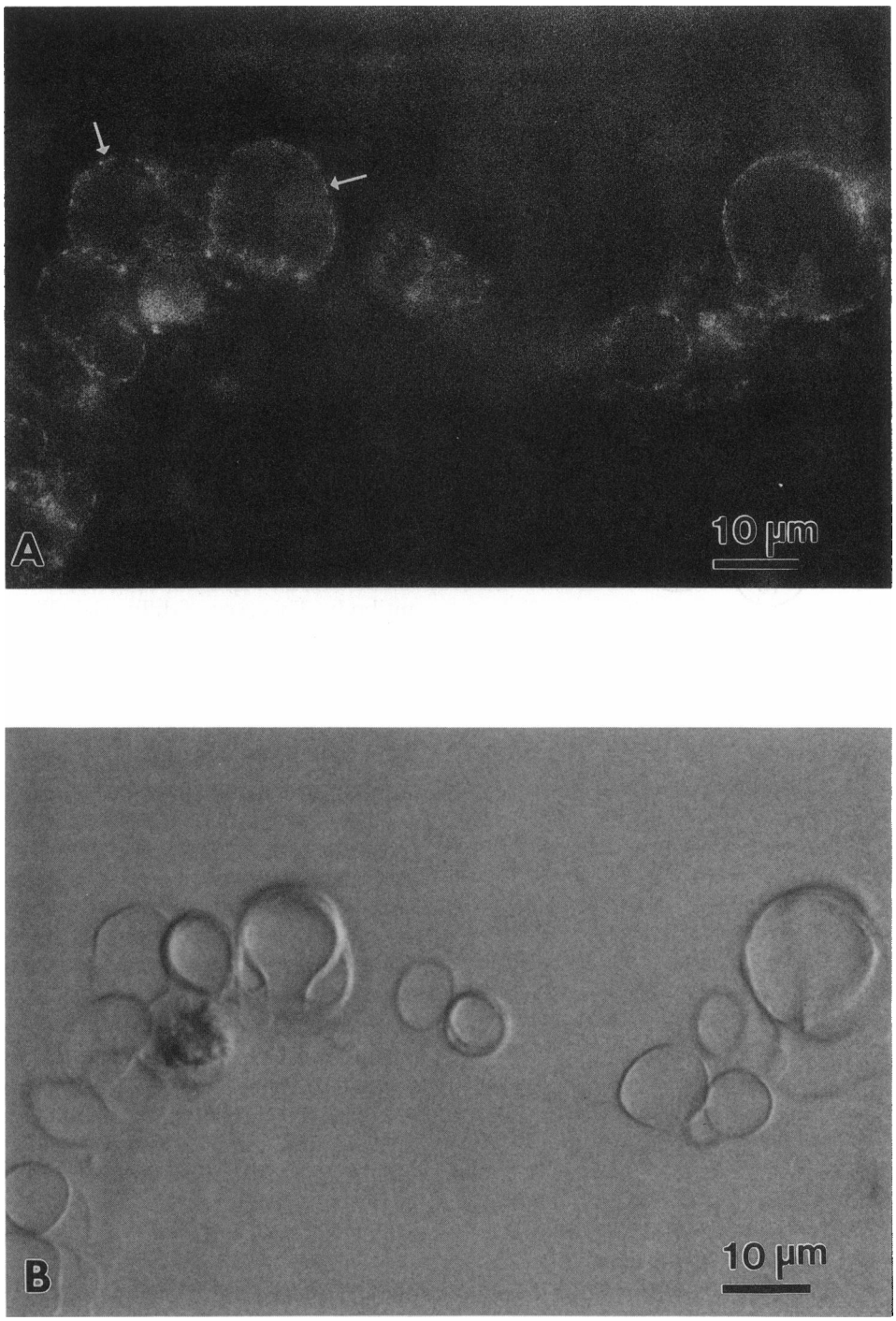

FIGURE 3 Temperature dependent patching of FITC-conjugated GAR antibody on giant liposomes of Tanaka lipids containing SP-B(1-25) and PR anti-SP-B(1-25) (30°C): (*A*) epifluorescence image, arrows mark examples of patching, (*B*) DIC image.

pha helix can be oriented in the lipid bilayer so that the hydrophobic region is in contact with the hydrophobic lipid core and the charged region is interacting with polar headgroups and water. In this way, SP-B(1-25) initially interacts electrostatically with charged lipid bilayers and then orients in the bilayer so that its charged residues are exposed to the hydrophilic environment and may be bound by antibody.

Association of SP-B(49-66) with giant vesicles

Vesicles formed from Tanaka lipids and 3% SP-B(49-66) mixed in chloroform/methanol, dried on cover slips then hydrated, were not labelled by antibody to SP-B(49-66). As SP-B(49-66) contains more hydrophobic residues than SP-B(1-25) and is water insoluble, our results

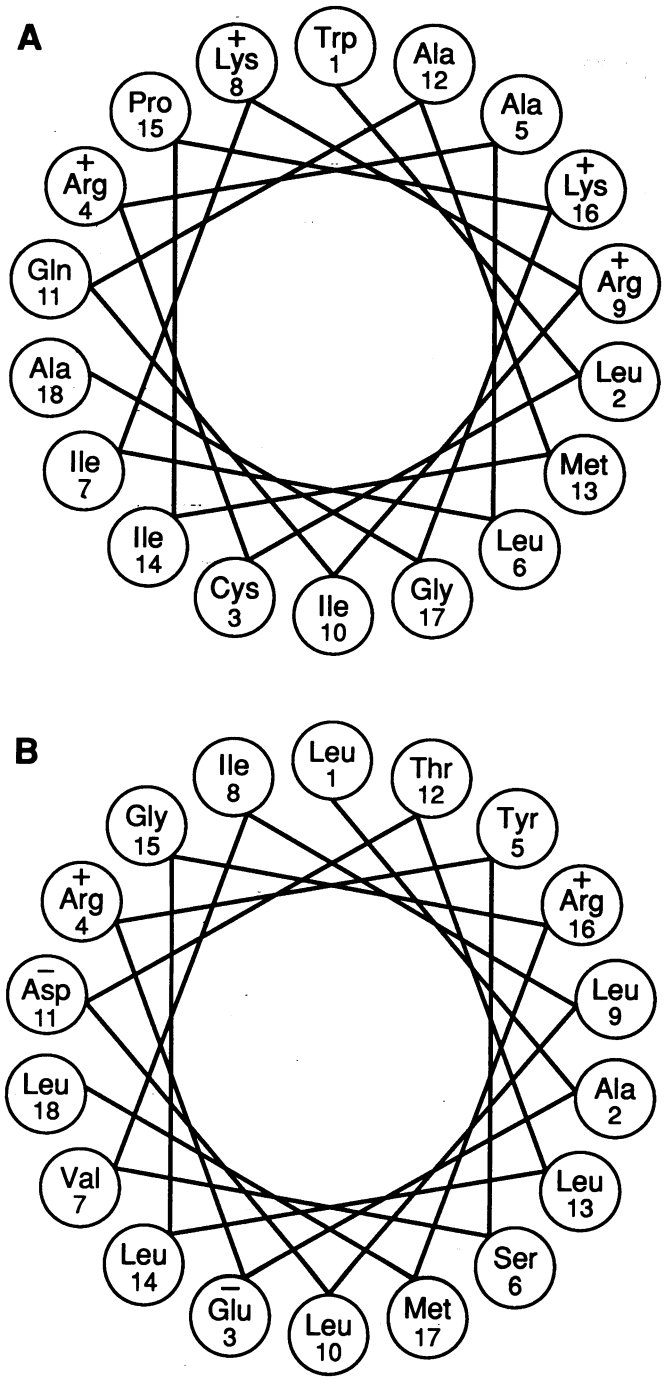

FIGURE 4 Edmundson helical wheel diagrams for (*A*) SP-B NH_2-terminal residues Trp-9 (position 1) to Ala-26 (position 18); (*B*) SP-B COOH-terminal residues Leu-49 (position 1) to Leu-66 (position 18). Symbols above residues indicate charge.

suggest that this peptide is more deeply embedded in the lipid bilayer. Due to its lack of water solubility, and its high affinity for lipids and nonpolar solvents, we are sure that the peptide is located within the vesicle bilayers, although it is not in contact with the lipid-water interface. Like the 1-25 region, the 49-66 region has a dominant alpha helical structure in a membrane mimic environment (24). Shiffer-Edmonson analysis of amino acid residues 49 through 66 is shown in Fig. 4 *B*. However, as there are two positively charged (arginine) and two negatively charged residues (aspartine and glutamine), the peptide has no net charge. Hence, the entire helix can be more deeply embedded in the lipid bilayer and it will be less accessible to antibody.

Accessibility of SP-B(1-78) to antibody

In order to test the surface accessibility of full length SP-B(1-78) protein domains in surfactant liposomes, liposomes were formed of Tanaka lipids and 3% of the 78 residue synthetic peptide. The liposomes were hydrated under reducing conditions with 5 mM dithiothreitol, such that the synthetic SP-B was noncovalently linked by disulfide bonds. Antibodies were then added as described above. Vesicles containing reduced SP-B(1-78) were not bound by 1-25 antibody. Diffuse fluorescence was associated with each vesicle labelled with antibody to SP-B(49-66) (Fig. 7; *arrows*), indicating that reduced SP-B(1-78) incorporated in vesicles is accessible to 49-66 antibody. This type of diffuse labelling was not observed in any other experiments. Note that the vesicles did not protrude from the lipid film under these reducing conditions. The next two experiments were identical to the first two except that dithiothreitol was absent in the buffer so that SP-B(1-78) was in its oxidized form. Vesicles containing oxidized SP-B(1-78) were not bound by 1-25 or 49-66 antibody.

Binding of the antibody against the NH_2-terminus does not occur with either reduced or oxidized synthetic SP-B(1-78) in immunostaining experiments either, suggesting that the lack of binding is more likely due to a difference in protein conformation rather than a variation in accessibility. On the other hand, the antibody to the COOH-terminus binds the full length SP-B(1-78) in immunostaining experiments, and binds weakly in a liposome environment. The 49-66 peptide, however, is not bound by antibody in a liposome environment. This suggests that the COOH-terminus region of the full monomeric synthetic SP-B(1-78) is more accessible to the bulk aqueous environment than the 49-66 peptide. Albumin is a known inhibitor of lung surfactant (39, 40). Therefore, to eliminate the possibility that albumin was somehow effecting the binding of antibody to SP-B, these experiments were repeated with no BSA in the buffer solution and the same results were obtained.

Relationship of vesicle shape to composition

Amphiphiles can form a variety of structures; for example, double chained surfactant molecules can assemble to form small spherical micelles, vesicles, tubules, or bilayers that can transform from one structure to another as temperature, counterions, and concentrations are varied (41–43). It is not surprising that hydrated mixtures of DPPC, DPPC/egg PG, DPPC/palmitic acid, and Tanaka lipids formed quite different structures at 25°C which

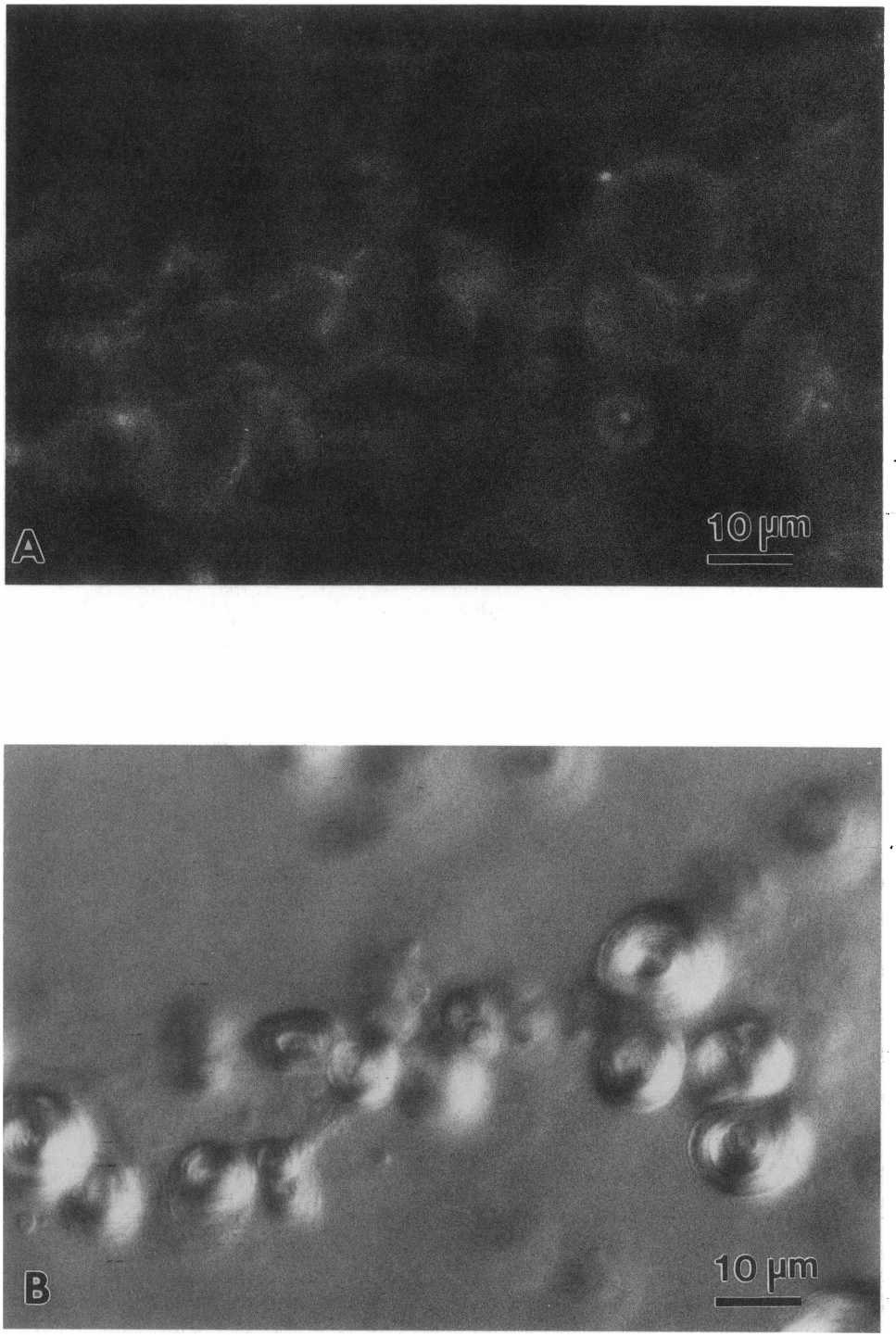

FIGURE 5 Weak binding of antibody (FITC-conjugated GAR antibody and PR anti-SP-B[1-25]) to SP-B(1-25) which had adsorbed to preformed DPPC vesicles: (*A*) epifluorescence, (*B*) DIC. Comparison of this image to Fig. 6 demonstrates that SP-B(1-25) adsorbs more readily to negatively charged lipid bilayers than neutral DPPC bilayers.

could easily be viewed in the microscope. DPPC formed multilayered structures ranging from ~4 to 30 μm (Fig. 8 *A; arrow*). DPPC/palmitic acid formed smaller (2 to 20 μm) and less densely packed structures that appeared to lie near the plane of the lipid film (Fig. 8 *B; arrow*). DPPC/egg PG and DPPC/egg PG/palmitic acid packed into spherical liposomes (Fig. 8, *C* and *D*). DPPC/egg PG liposomes appeared to constitute a bimodal population (vesicle size ranges from 4 to 30 μm); in one population, each liposome encapsulated many tightly packed vesicles that often extended close the center of the liposome (Fig. 8 *C; large arrow*) and the other population mainly consisted of vesicles that are unilamellar or encapsulated a few smaller vesicles (*small arrow*). DPPC/egg PG/pal-

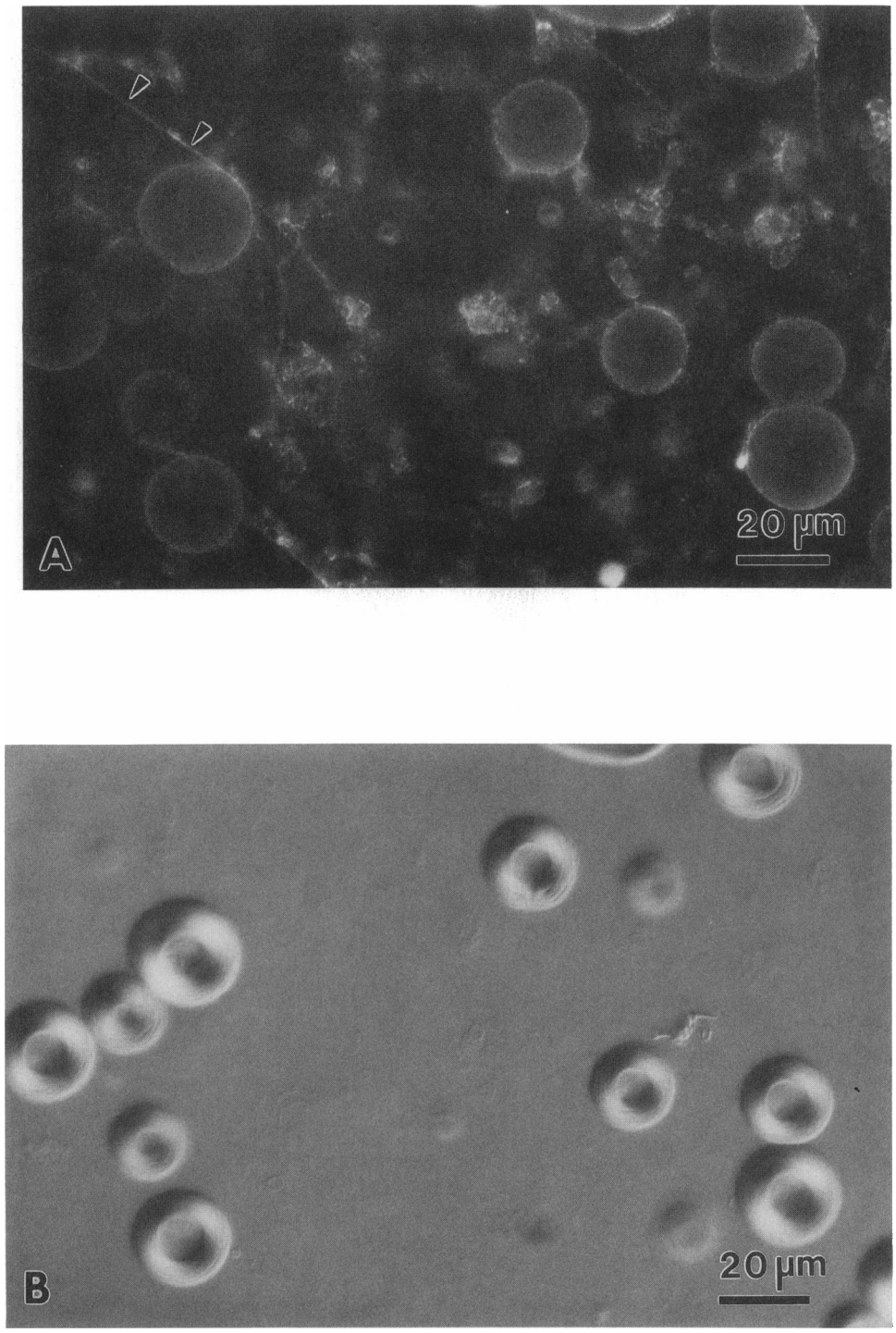

FIGURE 6 (*A*) Epifluorescence image of binding of antibody (FITC-conjugated GAR antibody and PR anti-SP-B[1-25] antibody) to SP-B(1-25) which had adsorbed to preformed DPPC/egg PG vesicles. Arrows mark fluorescence associated with tubular vesicles that were in a slightly different focal plane than the DIC image (*B*), thus only the corresponding multilamellar vesicles were imaged.

mitic acid liposomes consisted mainly of the later population and range in size from ~4 to 100 μm. SP-B(1-25) added after vesicle formation did not effect the shape of these mixtures. SP-B(1-25), SP-B(78), and SP-B(49-66) when included in the lipid film also had no effect. The shape and structure of the vesicles seemed to be dominated by the lipid behavior, and was relatively independent of the presence or absence of protein or peptide.

It is likely that much of this shape transformation effect can be accounted for by the lipid phase behavior of each lipid. DPPC is a zwitterionic lipid species; in the absence of charged interactions, interbilayer distances

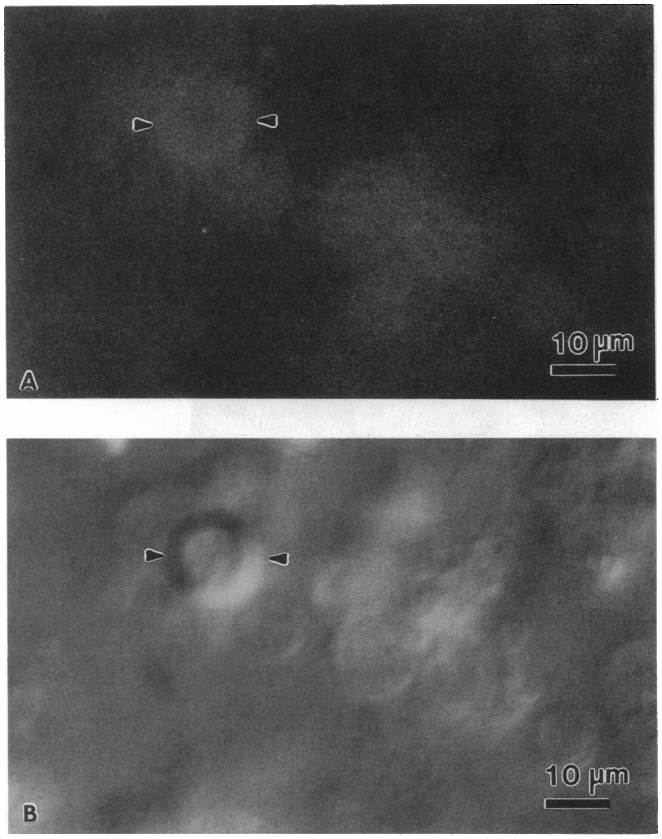

FIGURE 7 Weak and diffuse binding of antibody (FITC-conjugated GAR antibody and PR anti-SP-B[49-66] antibody) to reduced SP-B(1-78) associated with vesicles formed of Tanaka lipids. Arrows mark a corresponding vesicle in epifluorescence mode (*A*) and DIC (*B*). Note that the vesicles have a flattened appearance apparently due to the presence of the reducing agent (5 mM dithiothreitol).

are mainly limited by the short ranged repulsive hydration force (41, 44–46) and densely packed structures are formed. DSC studies indicate that palmitic acid packs well with DPPC and actually tends to raise the phase transition temperature (47, 48). Therefore, DPPC/PA vesicles were not hydrated above the gel-liquid crystalline phase transition temperature which begins at ~45°C for this mixture. This could have caused the formation of small aggregates. Egg PG had the most dramatic effect on the appearance of the vesicles. The hydrocarbon chain length and degree of unsaturation is inhomogeneous in egg PG. This type of inhomogeneity has a fluidizing effect on the lipid mixture, thus lowering the main phase transition temperature (41), so that the structures contained no sharp edges at room temperature. Additionally, because of the presence of negatively charged PG head groups, interbilayer distances are limited by longer ranged repulsive electrostatic interactions (49–51), resulting in less densely packed structures (42). It is possible that the egg PG preferentially partitioned into the mainly unilamellar vesicles. Addition of palmitic acid, which is greater than 99% negatively charged at pH 7.2 (pKa of ~5.0 [52, 53]), increased charge and possibly enhanced mixing. Due to interbilayer repulsion, encapsulated vesicles could no longer pack closely together and unilamellar vesicles were often formed.

This is the first time to our knowledge that the morphological features of the three lipid component Tanaka mixture have been compared with the binary mixtures. These observations are necessary because air-water interfacial adsorption measurements are often made using vesicle solutions spread at the interface or injected into the subphase (3, 7, 9, 15, 23, 27, 54). It has been shown that the Tanaka mixture spreads more quickly than any of the two component derivations and the addition of lung surfactant protein enhances surface adsorption (9). The tendency toward unilamellar vesicles may be an integral part of rapid spreading.

CONCLUSIONS

The amphipathic lung surfactant peptide, SP-B(1-25), localizes at the lipid bilayer surface of synthetic lung surfactant vesicles and is surface accessible to antibodies targeted against it. In addition, SP-B(1-25) (contains four positively charged amino acid residues) readily adsorbs to negatively charged lipid bilayers but is disinclined to adsorb to neutral vesicles. It appears that adsorption into a lipid bilayer involves an electrostatic attraction because adsorption to uncharged layers is weak. For antibody binding to occur, it is probable that the positively charged residues of SP-B(1-25) amphipathic alpha helix are exposed to the hydrophilic environment of the lipid headgroups and the hydrophobic residues interact with the lipid fatty acid chains. The location of SP-B(1-25) relative to the lipid bilayer, as well as its interaction with a negatively charged bilayer, may be an integral part of the enhanced effectiveness of synthetic lung surfactant containing SP-B(1-25) and negatively charged lipids. SP-B(49-66), when incorporated into giant vesicles, is not accessible to antibodies targeted against it from aqueous solution. Due to its lack of water solubility, and its high affinity for lipids and nonpolar solvents, we are sure that SP-B(49-66) is located within the vesicle bilayers, although it is not in contact with the lipid-water interface. Even though SP-B(49-66) forms an alpha helix in a lipid environment, its increased hydrophobicity should cause it to locate much more deeply within the hydrophobic interior of lipid bilayers than SP-B(1-25).

Only the COOH-terminal region (49-66 residues) of lipid associated monomeric SP-B(1-78) is accessible to antibody. The weak fluorescence associated with the antibody recognition suggests that SP-B(1-78) assumes certain orientations in the bilayer such that the COOH-terminus is accessible to the aqueous environment. In the monomeric form, the COOH-terminus residues 61-71 have a high hydrophobic moment (23). This additional amphipathicity may allow the COOH-terminus to orient near enough to the surface so that the 49-66 sequence of

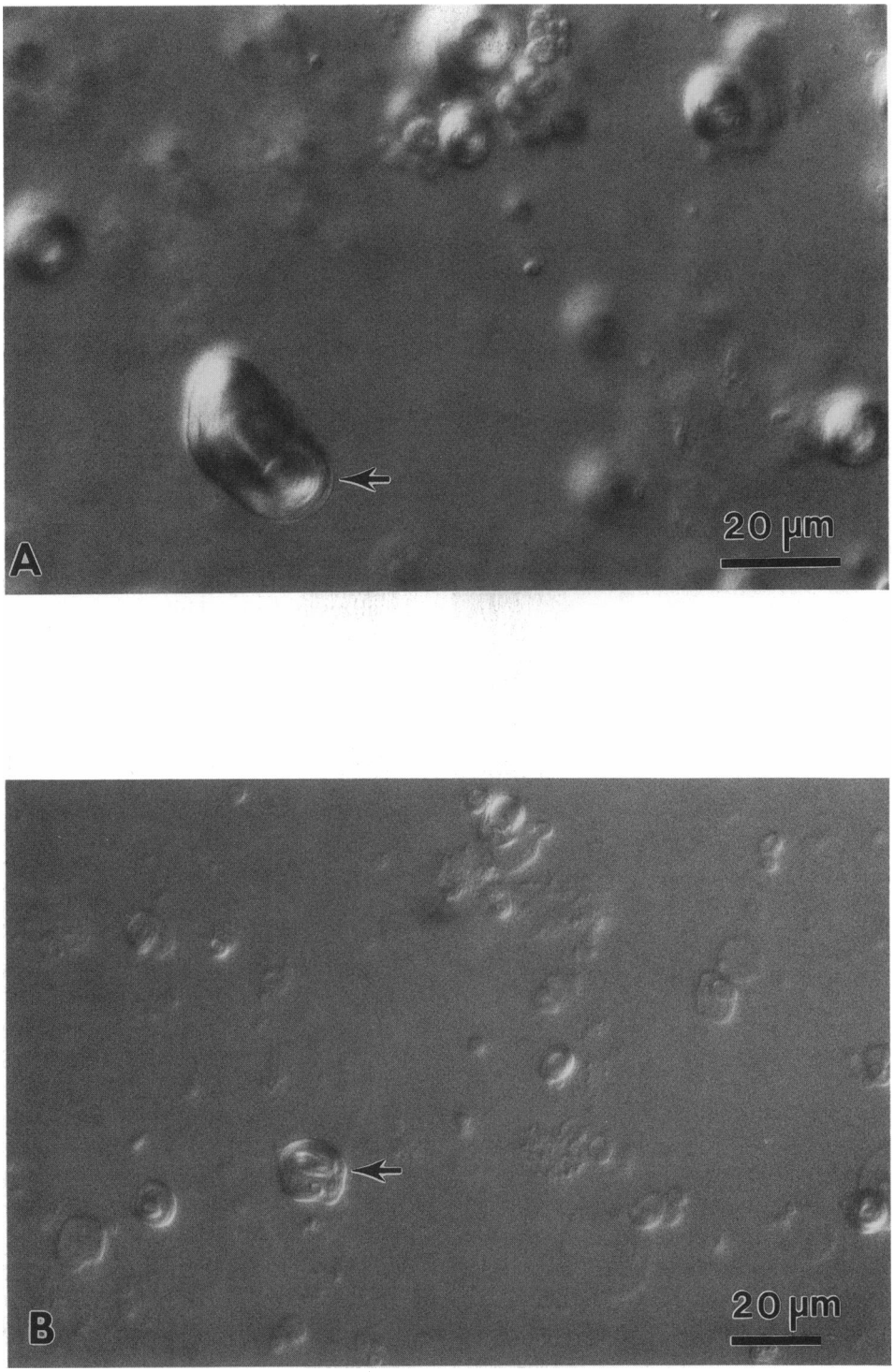

FIGURE 8 Liposome structures formed by mixtures of DPPC, DPPC/egg PG, DPPC/palmitic acid, DPPC/egg PG/palmitic acid hydrated in 10 mM PBS and 0.5% BSA. SP-B(1-25) added to the solution did not affect the appearance of the structures. Arrows mark typical structures. (*A*) DPPC formed multilayer structures. (*B*) DPPC/palmitic acid formed smaller and less densely packed structures. (*C*) DPPC/egg PG liposomes consisted of a bimodal population. The large arrow marks a typical example of large densely packed liposomes from one of the populations. The small arrow indicates a typical example of vesicles that are unilamellar or loosely encapsulate a few smaller vesicles that constituted the second population. (*D*) DPPC/egg PG/palmitic acid formed mainly unilamellar vesicles or vesicles containing a few entrapped vesicles.

the full synthetic protein is accessible to antibody, unlike the 49-66 peptide. Alternately, as the full synthetic protein also contains the surface-associated 1-25 sequence, the 49-66 sequence may be located more closely to the aqueous interface, allowing the weak binding we observed.

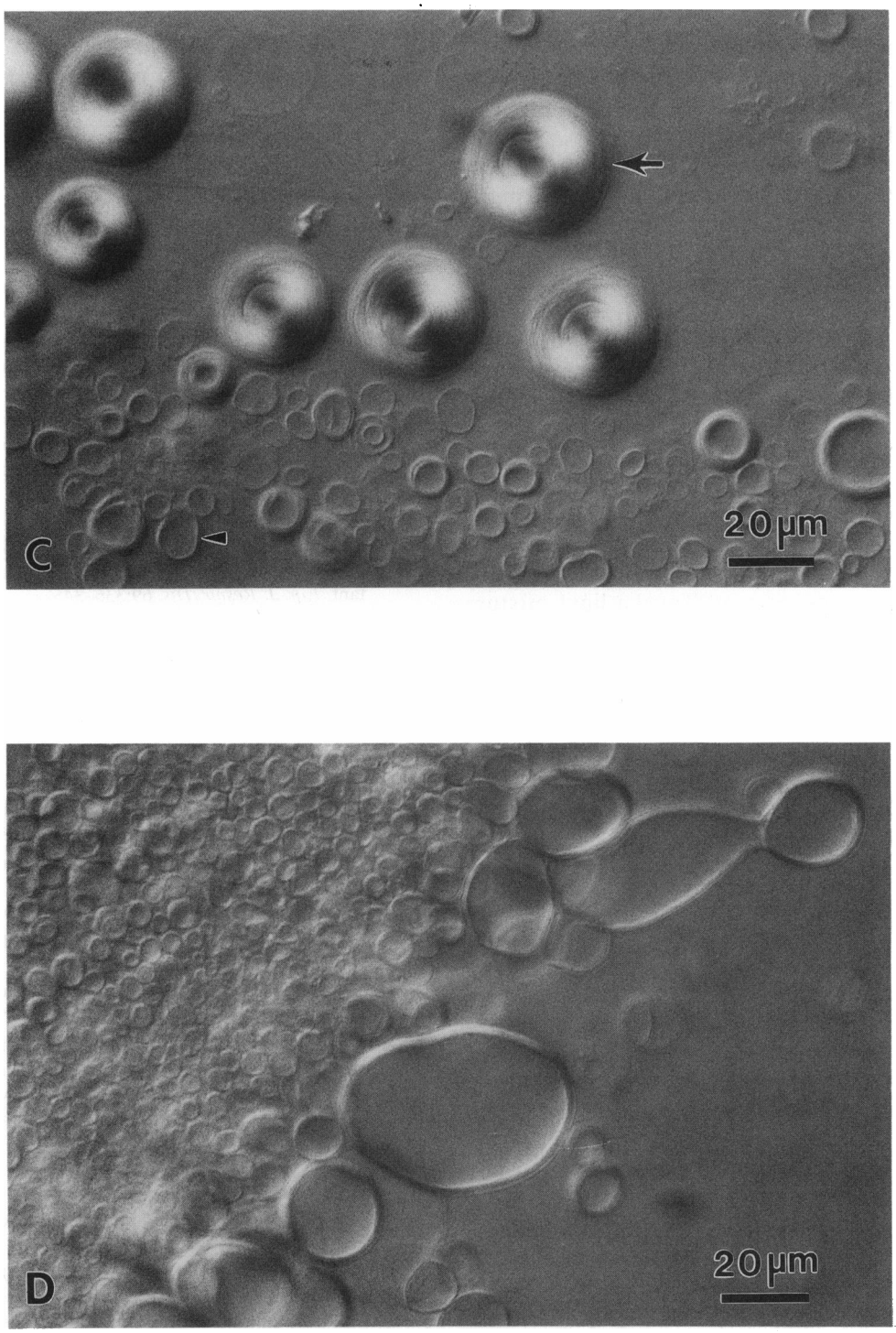

FIGURE 8 (continued)

We also observed that lipid associated monomeric and oligomeric SP-B(1-78) was not bound by the antibody to the 1-25 peptide. Preliminary immunostaining results also have shown that the 1-25 region of SP-B(1-78) is not bound by antibody to SP-B(1-25) peptide, most likely due to some conformation difference between the peptide and the full synthetic protein, and not to the surface accessibility of the protein in the bilayer. As a result of the amphipathic nature of the 1-25 region, we expect that this sequence is located in the bilayer in a similar fashion to the 1-25 peptide. However, the central region of SP-B(1-78) contains a high percentage of hydrophobic residues and may be interacting more strongly with the hydrophobic lipid core than the NH_2-terminus or

COOH-terminus. In future work, we plan a comparison of the binding characteristics of the synthetic SP-B(1-78) and native SP-B protein in lipid bilayers which should indicate differences in their conformation and topography in the lipid bilayer.

An advantage of this flow immunofluorescence technique is that the topography of peptide and protein molecules can be assessed in a realistic and flexible model membrane system of giant liposomes. In this system, it is convenient to change the composition of the lipid system, add components to solution (such as reductants and ions), and control the temperature of the system, while following the results visually. The binding of water soluble proteins to the lipid bilayer or antibody binding to lipid associated peptides or protein segments can be monitored according to changes made in the system in a simple and straightforward manner.

We have also been able to assess general morphological differences of vesicles formed from single components and binary mixtures of the Tanaka model surfactant. Only the three component Tanaka lipid mixture forms a population of mainly spherical unilamellar vesicles. The tendency to form unilamellar vesicles is certainly related to more rapid spreading of this mixture at an air-water interface compared with two component derivations of the Tanaka mixture that form multilamellar particles. The full synthetic protein or any of the peptide segments of SP-B do not appear to influence the number of vesicle layers or their configuration, so SP-B protein is likely to provide an additional mechanism (related to surface association of the 1-25 region with Tanaka lipid vesicles) to enhance adsorption to the air-water interface, as well as lowering surface tension.

We acknowledge helpful discussions with Dr. William Taeusch on lung surfactant proteins and their role in RDS treatments. We thank Dr. Kym Faull (of the University of California at Los Angeles) for mass spectral analysis of synthetic SP-B (1-78). The authors would also like to thank the members of Dr. Steven Fisher's laboratory at UCSB for helpful advice on fluorescence microscopy and the use of certain instruments, and Dr. Stuart Feinstein for the use of the fluorescence microscope.

This work was supported by a Whitaker Foundation Biomedical Engineering Grant (to Joseph Zasadzinski), National Institutes of Health grant HL-40666 (to W. Taeusch), and by a National Science Foundation grant (CTS90-15537) (to J. Zasadzinski). M. Longo was supported in part by a Patricia Robert Harris Fellowship and a Department of Education Fellowship from UCSB.

Received for publication 27 December 1991 and in final form 30 April 1992.

REFERENCES

1. King, R. J. 1984. Isolation and chemical composition of pulmonary surfactant. *In* Pulmonary Surfactant. E. Robertson, L. M. G. Van Golde, and J. J. Batenburg, editors. Elsevier, Amsterdam. 1–15.
2. Possmayer, F., S. H. Yu, J. M. Weber, and P. G. R. Harding. 1984. Pulmonary surfactant. *Can. J. Biochem. Cell Biol.* 62:1121–1133.
3. Shiffer, K., S. Hawgood, N. Duzgunes, and J. Goerke. 1988. Interactions of the low molecular weight group of surfactant-associated proteins (SP 5-18) with pulmonary surfactant lipids. *Biochemistry.* 27:2689–2695.
4. Persson, A., K. Rust, D. Chang, M. Moxley, W. Longmore, and E. Crouch. 1988. CP4: a pneumocyte-derived collagenous surfactant associated protein. Evidence for heterogeneity of collagenous proteins. *Biochemistry.* 27:8576–8584.
5. Possmayer, F. 1988. A proposed nomenclature for pulmonary surfactant-associated proteins. *Am. Rev. Respir. Dis.* 138:990–998.
6. Mathialagan, N., and F. Possmayer. 1990. Low-molecular weight hydrophobic proteins from bovine pulmonary surfactant. *Biochim. Biophys. Acta.* 1045:121–127.
7. Notter, R. H., D. L. Shapiro, B. Ohning, and J. A. Whitsett. 1987. Biophysical activity of synthetic phospholipids combined with purified lung surfactant 6,000 dalton apoprotein. *Chem. Phys. Lipids.* 44:1–17.
8. Suzuki, Y., T. Curstedt, G. Grossman, T. Kobayashi, R. Nilsson, K. Nohara, and B. Robertson. 1986. The role of the low-molecular weight (≤15,000-daltons) apoproteins of pulmonary surfactant. *Eur. J. Respir. Dis.* 69:336–345.
9. Tanaka, Y., T. Takei, T. Aiba, A. Kazus, K. Akira, and T. Fujiwara. 1986. Development of synthetic lung surfactants. *J. Lipid Res.* 27:475–485.
10. Tanaka, Y., T. Takei, Y. Kanazawa. 1983. Lung surfactants II. Effects of fatty acids, triacylglycerols and protein on the activity of lung surfactant. *Chem. Pharm. Bull.* 31:4100–4109.
11. Egan, E. A., R. H. Notter, M. S. Kwong, and D. L. Shapiro. 1983. Natural and artificial lung surfactant replacement therapy in premature lambs. *J. Appl. Physiol.* 55:875–83.
12. Fijiwara, T. 1984. Surfactant replacement in neonatal RDS. *In* Pulmonary Surfactant. E. Robertson, L. M. G. Van Golde, and J. J. Batenburg, editors. Elsevier, Amsterdam. 479–503.
13. Taeusch, H. W., K. M. W. Keough, M. Williams, R. Slavin, E. Steele, A. S. Lee, D. Phelps, N. Kariel, J. Floros, and M. E. Avery, 1986. Characterization of bovine surfactant for infants with respiratory distress syndrome. *Pediatrics.* 77:572–581.
14. Hawgood, S., B. J. Benson, J. Schilling, D. Damm, J. A. Clements, and R. T. White. 1987. Nucleotide and amino acid sequences of pulmonary surfactant protein SP 18 and evidence for cooperation between SP 18 and SP 28-36 in surfactant lipid adsorption. *Proc. Natl. Acad. Sci. USA.* 84:66–70.
15. Smith B., H. W. Taeusch, D. S. Phelps, and K. M. W. Keough. 1988. Mixtures of low molecular weight surfactant proteins and dipalmitoyl-phosphatidylcholine duplicate effects of pulmonary surfactant in vitro and in vivo. *Pediatr. Res.* 23:484–490.
16. Suzuki, Y., Y. Fujita, and K. Kogishi. 1989. Reconstitution of tubular myelin from synthetic lipids and proteins associated with pig pulmonary surfactant. *Am. Rev. Respir. Dis.* 140:75–81.
17. Takahashi, A., and T. Fujiwara. 1986. Proteolipid in bovine lung surfactant: its role in surfactant function. *Biochem. Biophys. Res. Commun.* 135:527–532.
18. Glasser, S. W., T. R. Korfhagen, T. E. Weaver, T. Pilot-Mathias, T. Fox, and J. A. Whitsett. 1987. cDNA and deduced amino acid sequence of human pulmonary surfactant associated proteolipid SPL(Phe). *Proc. Natl. Acad. Sci. USA.* 84:4007–4011.
19. Glasser, S. W., T. R. Korfhagen, T. E. Weaver, J. C. Clark, T. Pilot-Mathias, J. Meuth, L. J. Fox, and J. A. Whitsett. 1988. cDNA deduced polypeptide structure and chromosomal assignment of human pulmonary surfactant proteolipid, SPL, (pVal). *J. Biol. Chem.* 263:9–12.

20. Jacobs, K. A., D. S. Phelps, R. Steinbrink, J. Fisch, R. Kriz, L. Mitsock, J. Dougherty, H. W. Taeusch, and J. Floros. 1987. Isolation of a cDNA clone encoding a high molecular weight precursor to a 6-kDa pulmonary surfactant-associated protein. *J. Biol. Chem.* 262:9808–9811.

21. Warr, R. G., S. Hagwood, D. I. Buckley, T. M. Crisp, J. Schilling, B. J. Benson, P. L. Ballard, J. A. Clements, and R. T. White. 1987. Low molecular weight human pulmonary surfactant protein (SP5): isolation, characterization and cDNA and amino acid sequences. *Proc. Natl. Acad. Sci. USA.* 84:7915–7919.

22. Bruni, R., H. W. Taeusch, and A. J. Waring. 1991. Surfactant protein B: lipid interactions of synthetic peptides representing the amino-terminal amphipathic domain. *Proc. Natl. Acad. Sci. USA.* 88:7451–7455.

23. Waring, A., W. Taeusch, R. Bruni, J. Amirkhanian, B. Fan, R. Stevens, and J. Young. 1989. Synthetic amphipathic sequences of surfactant protein-B mimic several physiochemical and in vivo properties of native pulmonary surfactant proteins. *Peptide Res.* 2:308–313.

24. Fan, B. R., R. Bruni, H. W. Taeusch, R. Findlay, and A. J. Waring. 1991. Antibodies against synthetic amphipathic helical sequences of surfactant protein SP-B detect a conformational change in the native protein. *FEBS.* 282:220–224.

25. Waring, A. J., R. Stevens, J., Young, R., Bruni, and W. Taeusch. 1991. Reconstitution of a synthetic peptide resembling protein SP-B in phospholipid dispersions: structure-activity correlations. *Biophys. J.* 59:507*a*. (Abstr.)

26. Eisenberg, D., R. M. Weiss, T. C. Terwilliger, and W. Wilcox. 1982. Hydrophobic moments and protein structure. *Faraday Symp. Chem. Soc.* 17:109–120.

27. Takahashi, A., A. J. Waring, J. Amirkhanian, B. Fan, and H. W. Taeusch. 1990. Structure-function relationship of bovine pulmonary surfactant proteins: SP-B and SP-C. *Biochim. Biophys. Acta.* 1044:45–49.

28. Parker, J. M., D. Guo, and R. S. Hodges. 1986. New hydrophilicity scale derived from high performance liquid chromatography peptide retention data: correlations of predicted surface residues with antigenicity and x-ray derived accessible sites. *Biochemistry.* 25:5425–5432.

29. Lerner, R. A. 1982. Tapping the immunological repertoire to produce antibodies of predetermined specificity. *Nature (Lond.).* 299:592–596.

30. Burnette, W. N. 1980. "Western blotting": electrophoretic transfer of proteins from sodium dodecyl sulfate-polyacrylamide gels to unmodified nitrocellulose and radiographic detection with antibody and radioiodinated protein A. *Anal. Biochem.* 112:195–203.

31. Gordon, R. D., W. E. Fieles, D. L. Schotland, R. Hogue-Angeletti, and R. L. Barchi. 1987. Topographical location of the C-terminal region of the voltage dependent sodium channel from electrophorous electricus using antibodies raised against a synthetic peptide. *Proc. Natl. Acad. Sci. USA.* 84:308–312.

32. Jennings, M. L. 1989. Topography of membrane proteins. *Annu. Rev. Biochem.* 58:999–1027.

33. Seckler, R., T. Moroy, J. Keith Wright, P. Overath. 1986. Antipeptide antibodies and proteases as structural probes for the lactose/H^+ transporter of escherichia coli: a loop around amino acid residue 130 faces the cytoplasmic side of the membrane. *Biochemistry.* 25:2403–2409.

34. Stewart, J. M., and J. D. Young. 1984. Solid Phase Peptide Synthesis, Second Edition. Pierce Chemical Co., Rockford, IL.

35. Briand, J. P., S. Muller, and M. H. V. Van Regenmortel. 1985. Synthetic peptides as antigens: pitfalls of conjugation methods. *J. Immunol. Methods.* 78:59–69.

36. Decher, G., H. Ringsdorf, J. Venzmer, D. Bitter-Suermann, and C. Weisgerber. 1990. Giant liposomes as model membranes for immunological studies: spontaneous insertion of purified K1-antigen (poly-α-2,8-NeuAc) of Escherichia coli. *Biochim. Biophys. Acta.* 1023:357–364.

37. Small, D. M. 1986. Handbook of Lipid Research 4. The Physical Chemistry of Lipids. Donald J. Hanahan, editor. Plenum Press, New York. 475–522.

38. Segrest, J. P., H. De Loof, J. G. Dohlman, C. G. Brouillette, and G. M. Anantharamaiah. 1990. Amphipathic helix motif: classes and properties. *Proteins.* 8:103–107.

39. Cockshutt, A. M., J. Weitz, and F. Possmayer. 1990. Pulmonary surfactant-associated protein A enhances the surface activity of lipid extract and reverses inhibition by blood proteins in vitro. *Biochemistry.* 29:8424–8429.

40. Fuchimukai, T. Fujiwara, A. Takahashi, and G. Enhorning. 1987. Artificial pulmonary surfactant inhibited by proteins. *J. Appl. Physiol.* 62:429–437.

41. Israelachvili, J. N. 1985. Intermolecular and surface forces. Academic Press Inc., Orlando, Florida. 246–264.

42. Madden, T. D., C. P. S. Tilock, K. Wong, and P. R. Cullis. 1988. Spontaneous vesiculation of large multilamellar vesicles composed of saturated phosphatidylcholine and phosphatidylglycerol mixtures. *Biochemistry.* 27:8724–8730.

43. Miller, D. D., J. R. Bellare, D. F. Evans, Y. Talmon, and B. W. Ninham. 1987. Meaning and structure of amphiphilic phases: inferences from video-enhanced microscopy and cryotransmission electron microscopy. *J. Phys. Chem.* 91:674–685.

44. Le Neveu, D. M., R. P. Rand, V. A. Parsegian, and D. Gingell. 1977. Measurement and modification of forces between lecithin bilayers. *Biophys. J.* 18:209–232.

45. Marra, J., and J. Israelachvili. 1985. Direct measurements of forces between phosphatidylcholine and phosphatidylethanolamine bilayers in aqueous electrolyte solutions. *Biochemistry.* 25:4608–4618.

46. McIntosh, T. J., and S. A. Simon. 1986. Hydration and bilayer deformation: a reevaluation. *Biochemistry.* 25:4058–4066.

47. Mabrey, S., and J. M. Strurtevant. 1977. Incorporation of saturated fatty acids into phosphatidylcholine bilayers. *Biochim. Biophys. Acta.* 486:444–450.

48. McElhaney, R. 1982. The use of differential scanning calorimetry and differential thermal analysis in studies of model and biological membranes. *Chem. Phys. Lipids.* 30:229–259.

49. Cowley, A. C., N. L. Fuller, R. P. Rand, and V. A. Parsegian. 1978. Measurements of repulsive forces between charged phospholipid bilayers. *Biochemistry.* 17:3163–3168.

50. Marra, J. 1986. Direct measurement of the interactions between phosphatidylglycerol bilayers in aqueous electrolyte solution. *Biophys. J.* 50:815–825.

51. McIntosh, T. J., A. D. Magid, and S. A. Simon. 1990. Interactions between charged, uncharged and zwitterionic bilayers containing phosphatidylglycerol. *Biophys. J.* 57:1187–1197.

52. Garvin, J. E., and M. L. Karnovsky. 1956. The titration of some phosphatides and related compounds in nonaqueous medium. *J. Biol. Chem.* 221:211–222.

53. White, J. R. 1950. Dissociation constants of higher alkyl phosphate esters, phosphoric acids, phosphorous acids, phosphinic acids and carboxilic acids. *J. Am. Chem. Soc.* 72:1859–1860.

54. Jobe, A., and M. Ikegami. 1987. Surfactant for the treatment of respiratory distress syndrome. *Am. Rev. Respir. Dis.* 136:1256–1275.